

Habilitationsschrift

zur Erlangung der Venia Legendi
für das Fach Physik
der Ruprecht-Karls-Universität
Heidelberg

vorgelegt von

Kai Oliver Schweda
aus Heidelberg

2013

Prompt production of D mesons with ALICE at the LHC

Contents

1	Introduction	1
2	Results	7
2.1	Prompt production of D mesons in pp collisions	7
2.2	Prompt production of D mesons in Pb–Pb collisions	14
2.3	Correlations of charm and anti-charm quarks	21
3	Outlook	26
	References	28

1 Introduction

The Quark-Gluon Plasma (QGP) is the state of deconfined and thermalized QCD matter produced in high-energy nucleus-nucleus collisions. Its detailed characterization is a major long-term goal of the three large scale experiments ATLAS, CMS and ALICE using proton-proton, proton-lead and lead-lead collisions at unprecedented high energies provided by the Large Hadron Collider. In the standard Big Bang model, this QGP is the state of matter that permeated the early universe after the electro-weak phase transition, i.e. from picoseconds to about 10 microseconds after the Big Bang. A precise determination of its properties including critical temperature, degrees of freedom, speed of sound, and, in general, transport coefficients would be a major achievement, bringing a far better understanding of QCD as a genuine multi-particle theory.

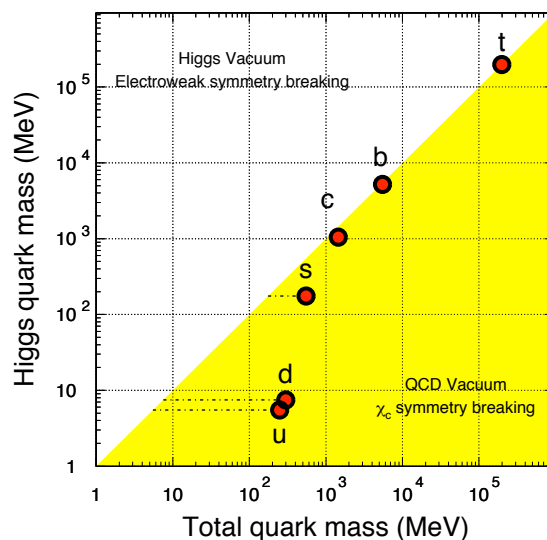


Figure 1.1: Quark masses in the QCD vacuum and the Higgs vacuum. A large fraction of the light quark masses arises due to chiral symmetry breaking in the QCD vacuum. This figure has been taken from [1].

ALICE successfully started data taking with Pb-Pb interactions in 2010. The experimental data set presently available, already allows for quantitative studies of rare probes, i.e. heavy-flavor particles, quarkonia, real and virtual photons, jets, and their correlations with other probes.

Heavy-flavor particles containing a heavy quark (charm or beauty) are unique probes for studies into QGP bulk properties. Their heavy mass constitutes a new scale in the system that is much larger than the QCD scale, $m_c, m_b \gg \Lambda_{\text{QCD}}$, making their production cross sections accessible to calculations in perturbative QCD. Their mass is also much larger than the maximum initial QGP temperature. Heavy quarks acquire their mass almost entirely from the electroweak sector due to their coupling to the Higgs field, see Fig. 1.1. Therefore, they remain heavy even when chiral symmetry is at least partially restored in a QGP. This makes heavy quarks a calibrated probe for studies of QGP bulk properties. They provide access to the degree of thermalization among quarks and gluons in the QGP. Heavy-quark elliptic flow is especially sensitive to the partonic equation of state, relating macroscopic QGP properties such as energy density, temperature and pressure. Ultimately, heavy quarks might fully equilibrate and become part of the strongly-coupled medium. Studying the in-medium heavy-quark energy-loss mechanism provides both a test and proving ground for the multi-particle aspects of QCD and a probe of the QGP density. In particular, it is crucial to characterize the dependences of energy loss on the parton color charge, mass, and energy, as well as on the density of the medium.

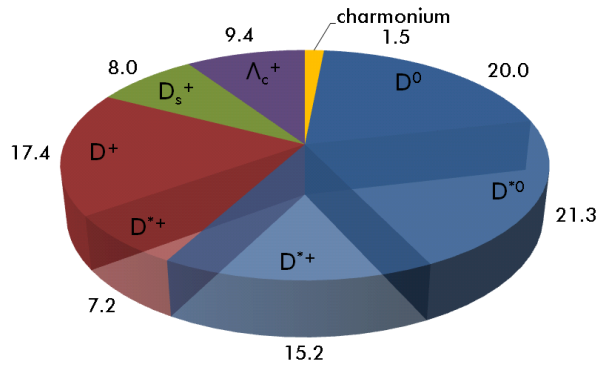


Figure 1.2: Relative abundances of charm quarks hadronizing into particular hadron species in vacuo. The contribution from the first excited states $D^*(2007)^0$ and $D^*(2010)^+$ to neutral (blue) and charged (red) D mesons is also indicated [2, 3]. The numbers given are in units of percent.

Experimental studies require the detection of charmed hadrons. The relative abundances of charm quarks hadronizing into a particular hadron species in vacuo are given in Fig. 1.2. The contributions from the first excited states $D^*(2007)^0$ and $D^*(2010)^+$ to

neutral and charged D mesons are also indicated. The contribution from higher resonances is less than 5%, and is neglected in the following. Throughout this thesis, ‘prompt’ refers to all D mesons not originating from weak decays such as $B \rightarrow D + X$. In particular, ground-state D mesons originating from the decay of excited charm resonances also belong to prompt production.

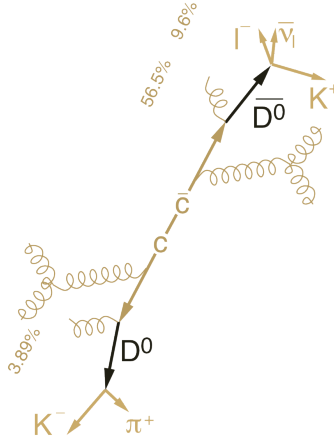


Figure 1.3: Schematic view of charm-quark hadronization and decay [2, 4]. The numbers indicate the probability of a charm quark hadronizing into a neutral D meson (56.5%) and the branching ratios for the pictured hadronic (3.89%) and semi-leptonic (9.6%) decay channels.

Charmed hadrons decay before they reach any active detector material. Thus they have to be reconstructed from their decay products. The production and decay of a charmed hadron is schematically shown in Fig. 1.3. A charm and an anti-charm quark are created in pairs in strong interactions, mostly due to gluon-gluon processes. Both charm quarks hadronize e.g. into a neutral D and \bar{D} meson, which decay at the secondary vertex after moving typically a fraction of a millimeter away from the primary collision vertex.

The detection of charmed hadrons through their semi-leptonic decays has the advantage of larger branching ratios and the possibility of triggering on high-momentum leptons. However, due to the decay kinematics, information on the charmed hadron momentum is largely lost [6]. Reconstructing charmed hadrons in their hadronic decay channels retains the full kinematic information, thus giving direct access to the modification of charmed hadron production in the QGP medium. Some properties of charmed hadrons and their decay modes are listed in Tab. 1.1.

meson	mass (MeV/ c^2)	$c\tau$ (μm) or Γ (keV)	decay mode	branching ratio (%)
D^0	1864.86 ± 0.13	122.9 ± 0.4	$K^- \pi^+$	3.88 ± 0.05
			$K^+ \pi^-$	$(1.47 \pm 0.07) \times 10^{-2}$
D^+	1869.62 ± 0.15	311.8 ± 0.2	$K^- \pi^+ \pi^+$	9.13 ± 0.19
D_s^+	1968.50 ± 0.32	149.9 ± 2.1	$K^- K^+ \pi^+$	5.49 ± 0.27
$D^*(2007)^0$	2006.99 ± 0.15	< 2100	$D^0 \pi^0$	61.9 ± 2.9
			$D^0 + \gamma$	38.1 ± 2.9
$D^*(2010)^+$	2010.29 ± 0.13	$83.3 \pm 1.2 \pm 1.4$	$D^0 \pi^+$	67.7 ± 0.5
			$D^+ \pi^0$	30.7 ± 0.5

Table 1.1: Some properties of D mesons [2, 5]. For the charmed resonances D^* , the natural line width Γ is given.

The hadrons's invariant mass is calculated using information from the detected decay daughter candidates. The charmed hadron yield then appears as a peak at the rest mass in the invariant mass distribution above a combinatorial background of uncorrelated particles. In order to enhance the signal-to-background ratio, excellent particle identification capabilities at low to intermediate momentum and precise sub-millimeter pointing resolution to the primary vertex are essential. In the ALICE apparatus [7], this is provided by the Time Projection Chamber (TPC) [8], which performs 3-dimensional tracking of charged particles and provides information on the specific energy deposit dE/dx in the TPC gas mixture. The resolution of the dE/dx measurement is close to the theoretical limit, i.e. it is dominated by intrinsic fluctuations of the energy deposit of charged particles when propagating in the TPC gas [8]. Particle identification is extended to intermediate momentum by the Time-of-Flight detector (TOF) [9], which uses multi-gap resistive plate chambers with an overall time resolution of 90 ps to separate kaons from pions on a track-by-track basis up to a momentum of 1.5 GeV/ c . Ultra-high spatial resolution is provided by the Inner Tracking System (ITS), which is based on silicon detector technology. Two inner layers of high-granularity active pixel sensors measure the daughter particles at a radial distance of 3.9 cm away from the primary vertex with an intrinsic resolution of 12 μm in the transverse plane, resulting in a pointing

resolution of $75 \mu\text{m}$ at the primary vertex for momenta larger than $1 \text{ GeV}/c$ [10].

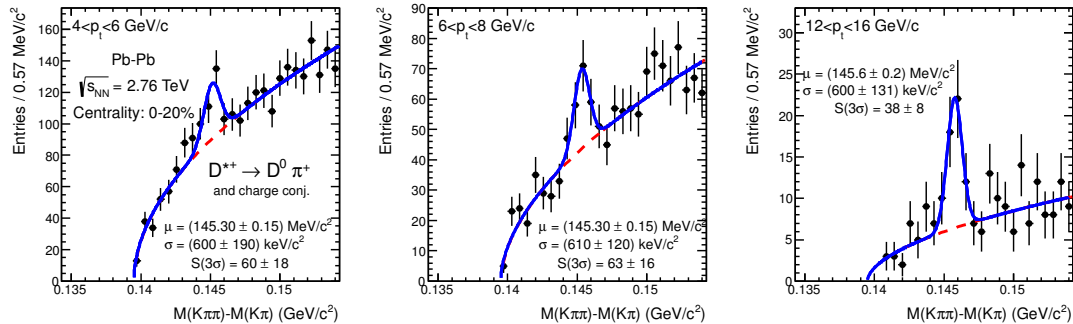


Figure 1.4: Invariant mass distribution of $D^*(2010)^+$ candidates from 20% most central Pb–Pb collisions at $\sqrt{s_{\text{NN}}} = 2.76 \text{ TeV}$ for different momentum bins. This figure has been taken from [11].

The invariant mass distribution of $D^*(2010)^+$ candidates from 20% most central Pb–Pb collisions at $\sqrt{s_{\text{NN}}} = 2.76 \text{ TeV}$ for different momentum bins is shown in Fig. 1.4. Note that the mass difference between the invariant mass of reconstructed $D^*(2010)^+$ and D^0 candidates is shown. Due to the small phase space available for the kinetic energy of the soft pion originating from the $D^*(2010)^+$ decay, the signal appears as a narrow peak at low invariant mass, close to the kinematic threshold. This leads to a small contribution from the combinatorial background. Since the daughter D meson is much heavier than the soft pion, in this representation the mass resolution is solely given by the momentum resolution of the soft pion. This results in a narrow width of the signal peak of less than 1 MeV , compared to typically 20 MeV for the other D mesons. Both the rather small contribution from the combinatorial background and the narrow signal peak make the statistical significance of the D^{*+} measurement practically identical to the D^0 measurement, with a higher momentum reach for the D^{*+} .

In this thesis, results from three decay modes for D mesons are reported, namely $D^0 \rightarrow K^- \pi^+$, with a branching ratio of $(3.88 \pm 0.05)\%$; $D^+ \rightarrow K^- \pi^+ \pi^+$, with a branching ratio of $(9.13 \pm 0.19)\%$; $D^*(2010)^+ \rightarrow D^0 \pi^+$, which strongly decays to D^0 with a branching ratio of $(67.7 \pm 0.5)\%$, and subsequently follows the channel $D^0 \rightarrow K^- \pi^+$; and their charge conjugates [2]. Strictly speaking, the invariant mass distribution for the decay $D^0 \rightarrow K^- \pi^+$ consists of the Cabibbo-favored decay $D^0 \rightarrow K^- \pi^+$ and the doubly Cabibbo-suppressed decay $\overline{D}^0 \rightarrow K^- \pi^+$. The latter has a branching ratio of $(1.47 \pm 0.07) \times 10^{-4}$,

and has been neglected. All cross sections reported are the sum for each D meson and its anti-particle divided by two. Contributions from the weak decays of B mesons are momentum-dependent, and amount to roughly 10 - 15%. These contributions have been subtracted by using results from state-of-the-art calculations in perturbative QCD. Results for D_s^+ production in proton-proton collisions can be found in [12]. Recent reviews of heavy-flavor production at collider energies and their implications for the properties of QCD matter are given in [13, 14].

This thesis is organized as follows. Results on charmed hadron production in proton-proton collisions with ALICE are presented in Sect. 2.1, and results from lead-lead collision are presented in Sect. 2.2. Model studies on charm anti-charm correlations and their implications on thermalization in high-energy nucleus-nucleus collisions are discussed in Sect. 2.3. An outlook is given in Sect. 3.

2 Results

2.1 Prompt production of D mesons in pp collisions

The measurement of charm and beauty production cross sections in proton–proton (pp) collisions at the Large Hadron Collider (LHC) constitutes a challenge to our understanding of calculations in perturbative Quantum Chromo–Dynamic (pQCD) at the highest collider energies. These calculations use the factorization approach to describe heavy-flavor hadron production as a convolution of three terms: the parton distribution function, the hard parton scattering cross section and the fragmentation function. The parton distribution function describes the initial distribution in Bjorken- x of quarks and gluons in the colliding protons. The hard parton scattering cross section is calculated as a perturbative series in terms of the coupling constant of the strong interaction. The fragmentation function parametrizes the relative production yield and momentum distribution for a heavy quark that hadronizes into a particular hadron species.

The production cross section of beauty hadrons at Tevatron at a collision energy of $\sqrt{s} = 1.96 \text{ TeV}$ [15–17] and at the LHC at $\sqrt{s} = 7 \text{ TeV}$ [18, 19] is well described by perturbative calculations at next-to-leading order, e.g. GM-VFNS [20, 21], or at fixed order with a next-to-leading-log resummation, i.e. FONLL [22, 23]. Charmed hadron production at Tevatron [24–26], at the LHC [27–29], and RHIC, e.g. the heavy-flavor decay lepton measurements at $\sqrt{s} = 200 \text{ GeV}$ [30, 31], are also reproduced by the pQCD calculations within experimental and theoretical uncertainties. On the other hand, the relative abundances of charmed hadrons test the statistical hadronization model [34] of charm quarks forming hadrons. If the hadronization of a charm quark occurs statistically, it should be independent of the collision system and energy. Finally, heavy-quark production rates in pp collisions provide an essential baseline for studies into the bulk properties of the Quark Gluon Plasma [35, 36].

The cross section for prompt production of D^{*+} mesons in pp collisions at $\sqrt{s} = 7 \text{ TeV}$ is shown in Fig. 2.1 as a function of transverse momentum. The spectrum starts at $1 \text{ GeV}/c$ and extends up to $24 \text{ GeV}/c$. At lower momenta, D mesons do not move far enough away from the primary vertex before the charm quark decays, and thus do not survive the topological selection. At the highest momenta, the invariant mass spectrum is essentially free of background and the measurement is solely restricted by statistics.

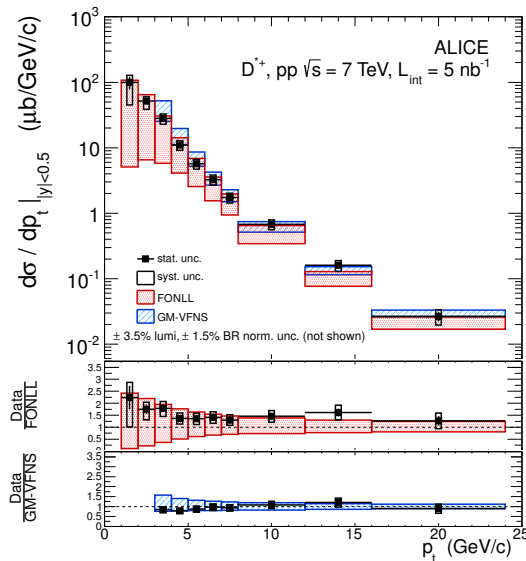


Figure 2.1: Cross section for prompt production of D^{*+} mesons in pp collisions at $\sqrt{s} = 7$ TeV and predictions from calculations in perturbative QCD within the FONLL [32] (red) and the GM-VFNS [33] (blue) framework. This figure has been taken from [27].

Predictions from calculations in perturbative QCD within the FONLL [32] (red) and the GM-VFNS [33] (blue) framework are shown by shaded areas. Both calculations use the CTEQ6.6 [37] next-to-leading-order parton distribution functions as input. The systematic uncertainties in each calculation scheme was estimated by simultaneously varying the factorization scale variable μ_F and the renormalization scale variable μ_R around their central value $\mu_F = \mu_R = \mu_0 = \sqrt{p_T^2 + m_c^2}$ by a factor of two with the constraint $0.5 \leq \mu_F/\mu_R \leq 2$. In the FONLL calculations, the charm quark mass was also varied around the central value of $m_c = 1.5 \text{ GeV}/c^2 \pm 0.2 \text{ GeV}/c^2$. Results from both calculations are able to describe the measurement within rather large uncertainties. Interestingly, all data points populate the upper band of results from FONLL. This behavior has already been observed at lower collision energies and different collision systems. On the other hand, compared to results from GM-VFNS, the data points sit on the lower side, which is at odds with observations at Tevatron energies. This indicates a steeper energy dependence in the GM-VFNS framework than in data.

In general, experiments only cover a small fraction of the full phase space populated by

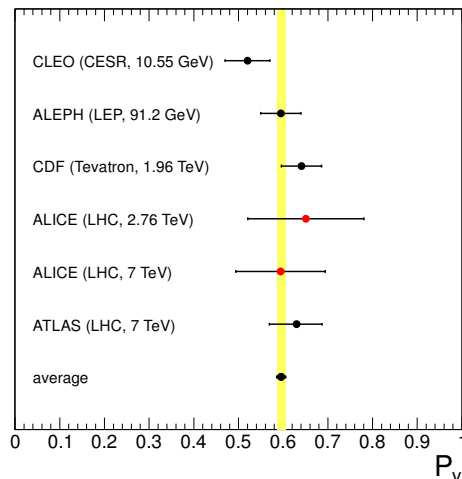


Figure 2.2: The fraction P_v of D mesons with valence quark content $|c\bar{d}\rangle$ created in a vector state over all D mesons with the same valence quark content [24,27,28, 38–41]. The weighted average of the experimental measurements reported in Ref. [42] and of the LHC data [27,28] shown in the figure is $P_v = 0.60 \pm 0.01$, and is represented by a solid yellow vertical band. This figure has been taken from [43].

charm production. For example, with the present limitation in $p_T > 1 \text{ GeV}/c$, ALICE covers about 70-80% of the transverse momentum spectrum at mid-rapidity and roughly 10% of the total production cross section for each D meson. Thus extrapolating the data by simply adding results from calculations in pQCD in the uncovered space phase would lead to results that are largely dominated by the calculations. Therefore, the relative distribution, i.e. the shape in transverse momentum and rapidity, is taken from the pQCD calculations to determine the fraction of charm production covered by the experiment. In the following, the default extrapolation method used by all high-energy experiments is described. For each D meson species, the total production cross section σ_D was extracted by multiplying the measured cross section by the ratio of the calculated total cross section over the calculated cross section in the experimentally covered phase space. The systematic uncertainties of the calculation were estimated by varying the renormalization (μ_R) and factorization (μ_F) scale variables and the charm quark mass (m_c), as described above. Uncertainties in the parton distribution functions were estimated using the CTEQ6.6 [37] PDF uncertainty eigenvectors and adding the

largest positive and negative variation in quadrature. Finally, all three contributions were added in quadrature.

One way of addressing charm quark hadronization is to consider the ratio of D mesons with valence quark content $|c\bar{d}\rangle$ created in a vector state (spin 1) to those produced in a vector (spin 1) or a pseudoscalar state (spin 0). This ratio, P_v , is calculated by taking the ratio of $\sigma_{D^{*+}}$ over the sum of $\sigma_{D^{*+}}$ and the part of σ_{D^+} not originating from D^{*+} decays,

$$P_v = \frac{\sigma_{D^{*+}}}{\sigma_{D^{*+}} + \sigma_{D^+} - \sigma_{D^{*+}} \cdot (1 - \text{BR}_{D^{*+} \rightarrow D^0 \pi^+})} = \frac{\sigma_{D^{*+}}}{\sigma_{D^+} + \sigma_{D^{*+}} \cdot \text{BR}_{D^{*+} \rightarrow D^0 \pi^+}}. \quad (2.1)$$

The advantage of this representation is that the right-hand side of Eq.(2.1) only contains one branching ratio with a small experimental uncertainty, while for the decay to D^+ two branching ratios either including a neutral pion or a photon would be required.

With the ALICE data, this results in

$$P_v(2.76 \text{ TeV}) = 0.65 \pm 0.10 (\text{stat.}) \pm 0.08 (\text{syst.}) \pm 0.002 (\text{BR})_{-0.003}^{+0.011} (\text{extr.}),$$

$$P_v(7 \text{ TeV}) = 0.59 \pm 0.06 (\text{stat.}) \pm 0.08 (\text{syst.}) \pm 0.002 (\text{BR})_{-0.002}^{+0.005} (\text{extr.}),$$

where uncertainties due to the extrapolation into the full phase space and branching ratios are negligible. These values coincide with results from other experiments at different collision energies and for different colliding systems [24, 27, 28, 38–41], as shown in Fig. 2.2. This means that the charm quark does not remember its origin and hadronizes independently of its production mechanism. In hindsight, this justifies the factorization ansatz to describe charmed-hadron production with the creation of a charm–anti-charm quark pair occurring at an early time scale and its hadronization at a later one.

The weighted average of the experimental measurements reported in Ref. [42], with average 0.594 ± 0.010 , with the LHC data [27, 28] shown in Fig. 2.2 is $P_v^{\text{average}} = 0.60 \pm 0.01$, which is represented by a solid yellow vertical band in the figure. Note that P_v can also be determined from the ratio of the ground-state D mesons D^0 and D^+ . This is due to the fact the excited state $D^*(2007)^0$ solely decays to D^0 due to energy conservation and $D^*(2010)^+$ decays to D^0 and D^+ with a ratio of roughly 2:1 due to isospin conservation, see Fig. 1.2. This leads to an asymmetry in the prompt production of D^0 and D^+ , i.e. a ratio different from unity.

The expectation from naïve spin counting amounts to $P_v^{\text{Spin counting}} = 3/(3+1) = 0.75$, which does not agree with data. The argument of naïve spin counting originates from heavy-quark effective theory (HQET) assuming an infinitely large heavy-quark mass, meaning that the effect due to the mass difference between D^{*+} and D^+ is negligible. With a relative mass difference of $\Delta m/m \approx 7.5\%$ in the D meson system, HQET is not a good assumption for the charm quark. This contrasts with the B meson system which has $\Delta m/m \approx 8.7\%$.

Calculations combining the Lund symmetric fragmentation function with exact Clebsch-Gordan coefficient coupling from the virtual quark–antiquark pair to the final hadron state functions predicts $P_v^{\text{Lund frag}} \approx 0.63$ [44], which is in good agreement with data. In this model, due to Clebsch-Gordan coefficient coupling, spin counting is automatic, while differences in the hadron mass are taken into account in the fragmentation function by an exponential term. On the other hand, in the Statistical Model [34,35], the ratio of the total yields of the directly-formed charmed mesons D^{*+} and D^+ , which have identical valence quark content, is expected to be $3 \cdot (m_{D^{*+}}/m_{D^+})^2 \cdot \exp(-(m_{D^{*+}} - m_{D^+})/T) \approx 1.4$ for a temperature parameter of $T = 164 \text{ MeV}$, where the factor of three comes from spin counting. We calculate $P_v^{\text{Stat. Model}} \approx 0.58 \pm 0.13$ for $T = (164 \pm 10) \text{ MeV}$. Other implementations of the Statistical Model [45, 46] predict similar values of P_v , ranging between 0.55 and 0.64. The experimental results for P_v thus allow for a description within the statistical hadronization of charm [34, 35] or calculations considering the Lund symmetric fragmentation function [44].

The total charm production cross section $\sigma_{c\bar{c}}$ was estimated for each species of D meson separately by dividing the total D meson production cross section σ_D by the relative production yield for a charm quark hadronizing to a particular species of D meson, that is the fragmentation fractions (FF) of 0.557 ± 0.023 for D^0 , 0.226 ± 0.010 for D^+ , and 0.238 ± 0.007 for D^{*+} [2]. The measured yields are consistent with these ratios. The weighted average of the total charm production cross section was then calculated from the extrapolated values for D^0 , D^+ , and D^{*+} .

The total nucleon-nucleon charm production cross section [28, 29, 47, 49, 51] and its dependence on the collision energy is shown in Fig. 2.3. The uncertainty boxes around the ATLAS [28] and ALICE [27] points denote the extrapolation uncertainties alone, while the uncertainty bars represent the overall uncertainties. Note that in case of

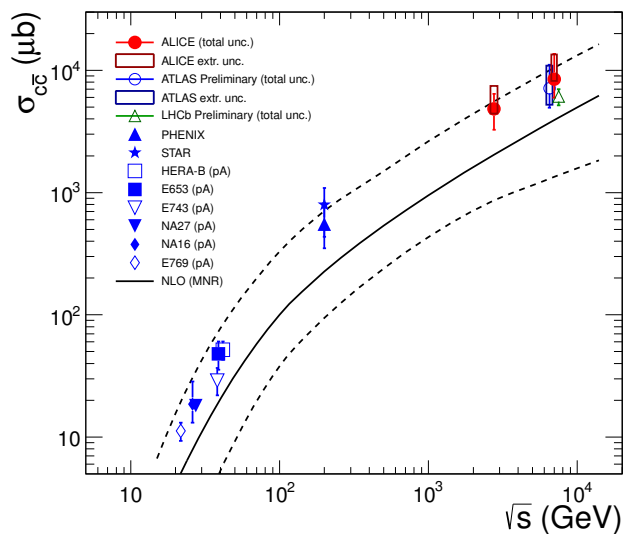


Figure 2.3: Total charm production cross section $\sigma_{c\bar{c}}$ per nucleon–nucleon pair versus collision energy [28, 29, 47–49]. In case of proton–nucleus (p–A) or deuteron–nucleus (d–A) collisions, the measured cross sections have been scaled down by the number of binary nucleon–nucleon collisions calculated in a Glauber model of the proton–nucleus or deuteron–nucleus collision geometry. Results from calculation in perturbative QCD [50] (and their uncertainties) are represented by solid (dashed) lines. This figure has been taken from [43].

proton–nucleus (p–A) or deuteron–nucleus (d–A) collisions, the measured cross sections have been scaled down by the number of binary nucleon–nucleon collisions calculated in a Glauber model of the proton–nucleus or the deuteron–nucleus collision geometry. At $\sqrt{s} = 7$ TeV, results from ALICE and preliminary measurements by the ATLAS [28] and the LHCb Collaboration [29] are in fair agreement. The curves show the calculations at next-to-leading-order within the MNR framework [50] together with their uncertainties using the same parameters (and parameter uncertainties) discussed above for FONLL. The dependence on the collision energy is described by pQCD calculations. Interestingly, all data points populate the upper band of the theoretical prediction. This might hint to a smaller actual charm quark mass than the central value of $m_c = 1.5$ GeV/ c^2 assumed in the pQCD calculations. A recent combined next-to-leading order QCD analysis of charm production in deep inelastic electron–proton scattering at HERA using the \overline{MS} running mass scheme determined a lower charm quark mass of $m_c \approx 1.26$ GeV/ c^2 [52]. A smaller

charm mass would implicitly lead to a larger cross section of gluons splitting into pairs of charm and anti-charm quarks. A deficit in gluon splitting processes to the production of charm has been indicated in Monte Carlo calculations when compared to measurements at Tevatron in the associated production of Z bosons with charm quark jets [53] and photon-tagged heavy-quark jets [54, 55] as well as at the LHC in the measurement of associated charm production in W final states [56].

2.2 Prompt production of D mesons in Pb–Pb collisions

Heavy quarks are almost exclusively produced in the initial stage of a collision in high-virtuality scattering processes, and their annihilation rate is small [57]. Hence, final state heavy-flavor hadrons at all transverse momenta originate from heavy quarks that have experienced all stages of the system’s evolution. Due to interactions with the medium, their production yields are sensitive to medium properties such as energy density, temperature, and in general transport properties. Heavy quarks lose energy through inelastic processes such as medium-induced gluon radiation [58, 59], and elastic processes such as collisions with other partons in the medium [60]. Since the color-charge factor of quarks is smaller than that of gluons, the energy loss of quarks should be smaller than for gluons. Additionally, the dead-cone effect reduces the available phase space for small-angle gluon radiation due to conservation of angular momentum [61] for heavy quarks at moderate energy-over-mass values [36, 62–65], leading to even smaller energy loss. However, other proposed mechanisms such as in-medium hadron formation and dissociation [66, 67] would lead to a larger energy loss of heavy-flavor hadrons, characterized by smaller formation times than for light-flavor hadrons. Ultimately, low-momentum heavy quarks might sufficiently interact with the medium constituents to even thermalize and become part of the medium, e.g. through re-scattering and in-medium resonant interactions [68].

The effects of parton energy loss, or in general medium effects, are quantified in the nuclear modification factor R_{AA} :

$$R_{AA}(p_T) = \frac{1}{\langle N_{\text{coll}} \rangle} \cdot \frac{dN_{AA}/dp_T}{dN_{pp}/dp_T} = \frac{1}{\langle T_{AA} \rangle} \cdot \frac{dN_{AA}/dp_T}{d\sigma_{pp}/dp_T}. \quad (2.2)$$

Here, $\langle T_{AA} \rangle$ is the average nuclear overlap function, as calculated in a Glauber model of the nucleus-nucleus collision geometry. For hard processes, production yields in nucleus-nucleus (AA) collisions are – in the absence of any nuclear medium effects – expected to scale with the number $\langle N_{\text{coll}} \rangle$ of binary nucleon-nucleon collisions when compared to pp yields. As a consequence, R_{AA} equals unity.

Heavy-quark masses are not negligible at momenta below $p_T \lesssim 10 \text{ GeV}/c$. A mass hierarchy in the nuclear modification factor R_{AA} value is expected when going from mostly gluon-originated light-flavor hadrons, e.g. pions, to D and B mesons (see e.g. [65, 70]), hence $R_{AA}^\pi < R_{AA}^D < R_{AA}^B$. Details depend on the reference spectrum from pp collisions.

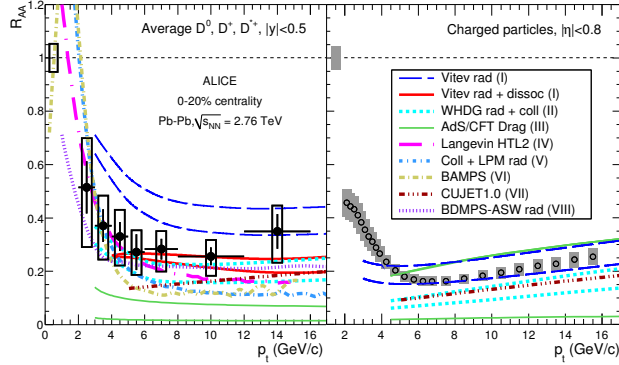


Figure 2.4: Nuclear modification factor R_{AA} of D mesons (left) and unidentified charged particles (right) and results from model calculations. This figure has been taken from [69].

A measurement and comparison of light versus heavy mass probes thus provides a unique test of the color-charge and mass dependence of parton energy loss.

The high statistics pp spectrum was obtained at a higher collision energy of $\sqrt{s} = 7$ TeV, which was the maximum possible collision energy in 2010. The pp reference spectrum for the R_{AA} measurements was obtained by scaling these results to the lower Pb–Pb collision energy of $\sqrt{s_{NN}} = 2.76$ TeV via a pQCD-driven approach. These results were validated by comparing to experimental data from a pp sample of limited statistics taken at the same collision energy [43]. The nuclear modification factor for D mesons, averaged over D^0 , D^+ , and D^{*+} , as measured by ALICE, is shown in the right panel of Fig. 2.4. The vertical bars represent statistical uncertainties in central collisions, having a typical magnitude of 20–25% for D^0 and 30–40% for D^+ and D^{*+} mesons. The results for the three D meson species numerically coincide within statistical uncertainties, exhibiting a suppression by a factor 3-4, i.e. $R_{AA} \approx 0.25$ –0.3, in central collisions for $p_T > 5$ GeV/c. For decreasing p_T , the nuclear modification factor of D^0 in central collisions tends to exhibit a lower suppression. Since charm is conserved, the depletion of the spectrum at large momentum should correspond to an enhancement at lower momentum. Also, if charm participates in the collective expansion of the medium, charm flow would lead to a depopulation at very low momentum and further enhance the spectrum at intermediate momentum. Both effects would lead to a nuclear modification factor above unity, with a maximum of $R_{AA} = 1.2 - 1.5$ around 2 GeV/c.

Besides parton energy loss, initial-state effects might also influence the R_{AA} measurement. In particular, a modification of the parton distribution functions in the nucleus when compared to the proton alters the initial hard scattering probability, thus affecting the production yields of hard partons, including heavy quarks. In the kinematic range relevant for charm production at LHC energies, the main predicted effect is nuclear shadowing, i.e. the reduction of the parton distribution functions for values of x below 10^{-2} . The effect of shadowing on the D meson R_{AA} was estimated using the next-to-leading order framework MNR [50] with the CTEQ6M parton distribution functions [71] for the proton and the EPS09NLO parametrization [72] for the lead nucleus. The effect from shadowing on the nuclear modification factor is estimated to be no larger than $\pm 15\%$ for $p_T > 6 \text{ GeV}/c$, indicating that the strong suppression observed in the data is a final-state effect.

The dependence on color charge and parton mass is investigated by comparing the nuclear modification factor of D mesons and π mesons. Since final results on the pion R_{AA} at the LHC were not available at the time of publication, a comparison is made with the measurement of unidentified charged particles which are dominated by pions. The average D meson nuclear modification factor is close to that of unidentified charged particles [73]. However, considering that the systematic uncertainties of D mesons are not fully correlated with p_T , there is an indication that $R_{AA}^D > R_{AA}^{\text{charged}}$. The nuclear modification factor of B mesons has been measured by the CMS Collaboration by detecting displaced J/ψ mesons with $p_T > 6.5 \text{ GeV}/c$ stemming from weak decays of B mesons [74]. Their suppression is clearly weaker than that of unidentified charged particles, while the comparison with D mesons is not yet conclusive.

Various models based on calculating parton energy loss may be used to compute the D meson nuclear modification factor. Here, a comparison is given between models, which can be divided into two groups:

- (A) models based on microscopic calculations in perturbative QCD, e.g. (I) - (VIII) [67, 70, 75–81]. Figure 2.4 displays the comparison of these models to the average D meson R_{AA} , for central Pb–Pb collisions (0–20%), along with the comparison to the charged-particle R_{AA} [73], for those models that also compute this observable: (I) [67], (II) [76], (III) [77], (VII) [81]. While the R_{AA} values vary drastically between different models, neither model is able to consistently describe the nu-

clear modification factor for light- and heavy-flavor hadrons. The apparent rise in R_{AA} with transverse momentum is solely due to the shape of the reference pp spectrum [82], and not a particular prediction of any model.

- (B) A recent development is the conjectured duality of quantum field theories of e.g. Yang-Mills-Shaw type, describing elementary particles on one side and theories of quantum gravity, formulated in string-theory, on the other [83]. The advantage is that while in quantum field theory the fields are strongly interacting and thus perturbative methods can not be applied, the fields in gravitational theory are weakly interacting, making calculations possible. A well studied case is the Anti-de-Sitter/conformal-field theory (AdS/CFT) correspondence. Here, string theory is formulated in an Anti-de-Sitter space with the conformal field theory living on the conformal boundary of the Anti-de-Sitter space-time. One specific example of the AdS/CFT correspondence relates the rather general class of type IIB string theories in ten-dimensional space that is defined by the the product of a five-dimensional Anti-de-Sitter-spacetime and a five-dimensional background, $AdS_5 \times S^5$, to $\mathcal{N} = 4$ supersymmetric Yang-Mills theory on the four-dimensional conformal boundary. The drag force of an external and thus infinitely heavy quark moving in a thermal plasma of a thermalized $\mathcal{N} = 4$ supersymmetric Yang-Mills theory has been calculated in such an approach [84]. A model determined drag coefficients (III) by incorporating experimental results from RHIC [77] and significantly underestimates the nuclear modification factor of D mesons.

The measurement of anisotropy in the azimuthal distribution of particle momenta provides further insight into the properties of the QGP medium. Anisotropic patterns originate from the initial anisotropy in the spatial distribution of the nucleons participating in the collision. The azimuthal anisotropy of produced particles is characterized by the Fourier coefficients $v_n = \langle \cos[n(\varphi - \Psi_n)] \rangle$, where n is the order of the harmonic, φ is the azimuthal angle of the particle, and Ψ_n is the azimuthal angle of the initial state symmetry plane for the n -th harmonic. For non-central collisions the overlap region of the colliding nuclei has a lenticular shape and the azimuthal anisotropy is dominated by the second Fourier coefficient v_2 , commonly denoted by elliptic flow [85, 86].

Two mechanisms are responsible for generating a non-zero v_2 . The first mechanism, dominant in the bulk, e.g. at low ($p_T < 3 \text{ GeV}/c$) and intermediate (3–6 GeV/c) trans-

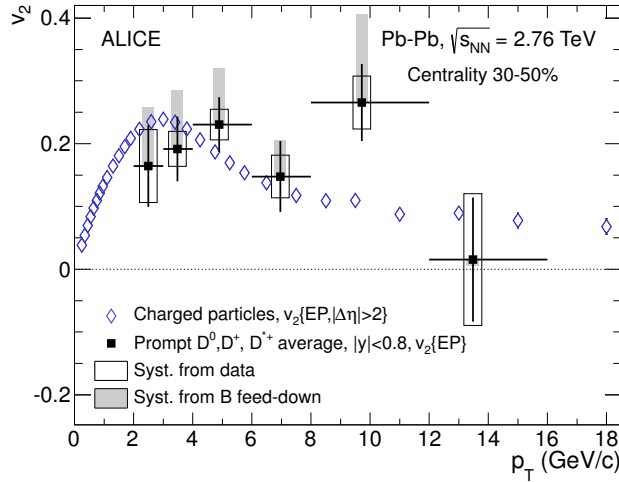


Figure 2.5: Elliptic flow coefficient v_2 for D mesons and unidentified charged particles. This figure has been taken from [11].

verse momentum, is the build-up of a collective expansion through interactions among the medium constituents. An anisotropic component in this collective expansion develops mainly in the early stages of the lifetime of the system, when the spatial anisotropy is large [87–89]. The second mechanism is the path-length dependence of in-medium parton energy loss, due to medium-induced gluon radiation and elastic collisions. This differential nuclear modification with respect to the reaction plane is predicted to give rise to a positive v_2 for hadrons up to large transverse momenta [90, 91]. The v_2 values measured for light-flavor hadrons at RHIC and LHC energies can be described for the low- p_T region in terms of collective expansion of a strongly-interacting fluid [85, 92–94], and for the high- p_T region ($p_T > 6$ – 8 GeV/ c) in terms of path-length dependent parton energy loss [76, 95–97].

The measurement of the elliptic flow of charmed hadrons provides further insight into the transport properties of the medium. At low p_T , charmed hadron v_2 offers a unique opportunity to test whether quarks with large mass ($m_c \approx 1.5$ GeV/ c^2) also participate in the collective expansion dynamics and possibly thermalize in the medium [6, 98]. Because of their large mass, charm quarks are expected to have a longer relaxation time, i.e. time scale for approaching equilibrium with the medium, with respect to light quarks [99]. At low and intermediate p_T , the D meson elliptic flow is expected to be sensitive to

the heavy-quark hadronization mechanism. If there are substantial interactions with the medium, a significant fraction of low- and intermediate-momentum heavy quarks could hadronize via combination with other quarks from the bulk of thermalized partons [100, 101], thus enhancing the v_2 of D mesons with respect to that of charm quarks [98]. In this context, the measurement of D meson v_2 is also relevant for the interpretation of the results on J/ ψ anisotropy [102], since J/ ψ mesons formed from $c\bar{c}$ combination would inherit the azimuthal anisotropy of their constituent quarks [103, 104]. At high p_T , the D meson v_2 can constrain the path-length dependence of parton energy loss, complementing the measurement of the suppression of particle yields with respect to the expectation from proton–proton collisions.

Theoretical models of heavy-quark interactions with the medium constituents enable the calculation of both the v_2 and R_{AA} of heavy-flavor mesons in a wide p_T range [78, 105–108]. For semi-central collisions at the LHC, they predict a large elliptic flow ($v_2 \approx 0.1$ – 0.2) for D mesons at $p_T \approx 2$ – 3 GeV/ c and a decrease to a constant value $v_2 \approx 0.05$ at high p_T .

The azimuthal anisotropy in heavy-flavor production was measured in Au–Au collisions at $\sqrt{s_{NN}} = 200$ GeV at RHIC using electrons from heavy-flavor decays. The resulting v_2 values are as large as 0.13 [109, 110].

For D mesons, the second Fourier coefficient, v_2 , was calculated according to:

$$v_2 = \frac{1}{R_2} \frac{\pi}{4} \frac{N_{\text{in-plane}} - N_{\text{out-of-plane}}}{N_{\text{in-plane}} + N_{\text{out-of-plane}}}. \quad (2.3)$$

Due to the limited statistics, the integrated asymmetry between the yields in the azimuthal range from $\phi = 0 - 90^\circ$ and $\phi = 90^\circ - 180^\circ$ was considered. The factor $\pi/4$ results from the integration of the second term, $2v_2 \cos(2\Delta\varphi)$, of the $dN/d\varphi$ distribution in the considered intervals of relative azimuth. The factor $1/R_2$ is the correction due to the angular resolution in determining the symmetry plane Ψ_2 [111], which smears out the angular modulation, leading to an apparent lower value for the observed v_2 .

The resulting D-meson v_2 is shown in Fig. 2.5. The average of the measured v_2 values in the interval $2 < p_T < 6$ GeV/ c is 0.204 ± 0.030 (stat) ± 0.020 (syst) $^{+0.092}_{-0}$ (B feed-down), which is larger than zero with 5.7σ significance. A positive v_2 is also observed for $p_T > 6$ GeV/ c , which most likely originates from the path-length dependence of the

partonic energy loss, although the large uncertainties do not allow a firm conclusion. The measured D meson v_2 is comparable in magnitude to that of charged particles, which are dominated by light-flavor hadrons [97]. This consistency suggests that the relaxation time of charm quarks in the medium is similar to that of light partons and it is short with respect to the time scale for diluting the initial geometrical anisotropy, possibly indicating that low momentum charm quarks take part in the collective motion of the system. The measured v_2 tends to favour the models that predict a larger anisotropy at low p_T [105–108]. Despite the relatively large uncertainties, these measurements on the nuclear modification factor and elliptic flow for D mesons together present the most stringent constraints to date on models describing the interaction of charm quarks with the QCD medium.

2.3 Correlations of charm and anti-charm quarks

The charm and beauty quantum numbers are conserved in strong interactions. Therefore, in strong interactions, heavy quarks are always created together with their anti-quark and are thus correlated. In collisions of leptons it has been shown that a hadron containing a charm or beauty quark carries a significant fraction of the initial quark momentum [112–114]. Hence, initial heavy-quark correlations survive the fragmentation process into hadrons to a large extent, and are observable e.g. in the angular distributions of pairs of D and \bar{D} mesons [47,115]. In pp collisions, the experimentally observed correlations of D mesons, measured at fixed target experiments [47] are reproduced well by the Monte Carlo event generator PYTHIA [116].

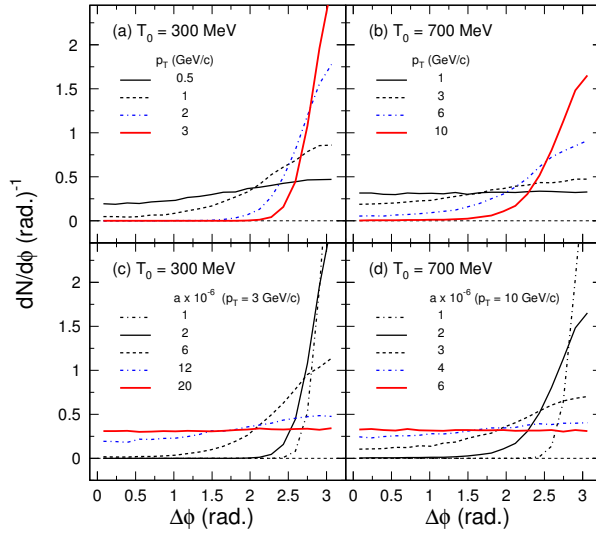


Figure 2.6: Correlations in relative azimuth $\Delta\phi$ of $D\bar{D}$ pairs from Langevin calculations with $T_0 = 300$ MeV (RHIC) and 700 MeV (LHC). The upper part shows the dependence of the correlations on the initial p_T of the charm quark; the lower part shows the drag coefficient dependence. This figure has been taken from [1].

In high-energy collisions of heavy nuclei, frequent interactions among partons (quarks and gluons) of the medium and heavy quarks may lead to a significant modification of these initially existing correlations. On the other hand, hadronic interactions at the late stage are insufficient to alter the azimuthal correlations of $D\bar{D}$ pairs [1]. Frequent

interactions distribute and randomize the available (kinetic) energy and finally drive the system, i.e. light quarks and gluons, to local thermal equilibrium. To what extent this also happens for heavy quarks is currently a subject of discussion [68, 117–120]. A decrease in the strength of heavy quark correlations in high-energy collisions of heavy nuclei as compared to pp collisions would indicate early thermalization also of heavy quarks.

We studied the modification of azimuthal correlations of D and \bar{D} meson pairs as a sensitive indicator of frequent occurrences of partonic scattering. To explore how the QCD medium generated in central ultra-relativistic nucleus-nucleus collisions influences the correlations of D and \bar{D} meson pairs, we employed a non-relativistic Langevin approach which describes the random walk of charm quarks in a QGP and was first described in Refs. [121–123],

$$\frac{d\vec{p}}{dt} = -\gamma(T)\vec{p} + \vec{\eta}(T), \quad (2.4)$$

with the drag coefficient γ and the normalized Gaussian noise variable $\vec{\eta}$ describing the heavy quark diffusion (random walk). The drag coefficient γ quantifies the resistance of the heavy quark in the QGP fluid. A large drag coefficient would lead to large heavy-quark flow. Both parameters are dependent on the local temperature of the system and were parameterized as in Ref. [121], e.g. $\gamma = aT^2$, neglecting any momentum dependence of the drag coefficient γ . They are related through the fluctuation-dissipation relation in equilibrium assuming a charm quark mass of $1.5 \text{ GeV}/c^2$.

In order to isolate the effects purely caused by parton-parton rescattering in the medium, charm and anti-charm quarks were generated with the same p_T and zero longitudinal momentum back-to-back, i.e. at relative azimuth $\Delta\phi = \pi$, and a delta function was used to fragment the charm quark into a charmed hadron at the hadronization stage.

Results for D meson (charm quark) pairs on their angular correlations are shown in Fig. 2.6 (a) for different initial charm quark p_T values, and $T_0 = 300 \text{ MeV}$, values typical for RHIC collisions. The fastest charm quarks, represented by the highest momenta, are able to escape from the QGP without suffering significant medium effects, while the slower quarks, represented by the lowest momenta, have their pair azimuthal correlation almost isotropic due to interactions in the medium.

Results for a higher initial temperature $T_0 = 700$ MeV, representative of LHC energies, are shown in Figure 2.6 (b). Here, interactions of charm quarks with the medium are so frequent that only the most energetic charm quarks preserve part of their initial angular correlation; low p_T pairs are even completely kinetically equilibrated and become part of the medium. Note that in the actual calculations, only longitudinal flow is considered. In reality, transverse radial flow leads to an enhancement of the same-side correlation [124] and will be present especially when interactions are frequent [117, 125, 126].

The above results were obtained with a drag coefficient estimated with perturbative QCD adopting a large coupling constant $\alpha_s = 0.6$ [127]. Recent pQCD calculations [128, 129] show a factor of 2-3 smaller drag coefficient. However, non-perturbative contributions that arise from quasi-hadronic bound states in the QGP might be important [129]. This would result in a much larger drag coefficient. Since exact values of the drag coefficient from lattice QCD calculations do not exist, the sensitivity on variations of the parameter a within the given range is considered. Figures 2.6 (c) and (d) show the drag coefficient dependence of the charm anti-charm angular correlations for high-energy charm quarks: $p_T = 3(10)$ GeV/ c and $T_0 = 300(700)$ MeV. The correlations dissipate when a is increased by around a factor of 5(2) with respect to the pQCD value.

At LHC energies, higher-order processes become dominant, and sensitivity to heavy quark thermalization might be lost. To overcome this complication, a two-particle transverse momentum correlator $\langle \Delta p_{t,1}, \Delta p_{t,2} \rangle$ was applied to pairs of heavy-quark hadrons and their semi-leptonic decay products as a function of their relative azimuth. This has the following advantages:

- (i) The correlator is sensitive to non-statistical fluctuations, thus scraping out any physical correlation.
- (ii) In case of physically uncorrelated candidate-pairs (e.g. combinatorial background), the extracted value for the correlator vanishes, thus providing a reliable baseline.
- (iii) A localization of the observed correlations in transverse momentum space may help to obtain further insight into the origin of the observed correlations in relative azimuth.

Calculations at leading order (LO) contain flavor creation processes ($q\bar{q} \rightarrow Q\bar{Q}$, $gg \rightarrow Q\bar{Q}$) and lead to an enhancement at relative azimuth around $\Delta\phi \approx 180^\circ$, i.e. the D meson pair is preferentially emitted back-to-back. In flavor excitation processes ($qQ \rightarrow qQ$, $gQ \rightarrow gQ$), one heavy quark from the proton sea participates in the hard scattering,

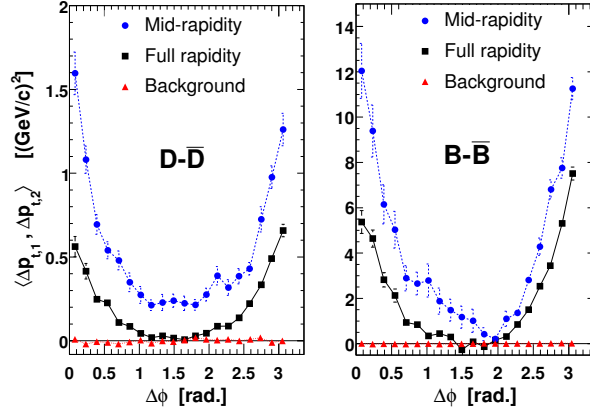


Figure 2.7: (Color online) Distribution of the momentum correlator $\langle \Delta p_{t,1}, \Delta p_{t,2} \rangle$ of $5 \cdot 10^5$ $D\bar{D}$ pairs (left panel) and $5 \cdot 10^5$ $B\bar{B}$ pairs (right panel) as a function of relative azimuth $\Delta\phi$ at mid-rapidity (circles), for full rapidity (squares) and for background using the mixed event method (triangles) for pp collisions at $\sqrt{s} = 14$ TeV as calculated using PYTHIA (6.406). This figure has been taken from [130].

leading to an asymmetry in momentum and the relative angular distribution. In gluon splitting processes ($g \rightarrow Q\bar{Q}$), one gluon splits into a heavy-quark pair with relatively small opening angle and transverse momentum. At even higher orders, the distinction becomes scale dependent and is thus less well-defined.

In order to extend calculations in PYTHIA beyond leading order, processes contributing at higher orders were calculated using a massless matrix element [131] applying a lower cut-off in the transverse momentum-transfer scale of the underlying hard scattering to avoid divergences in the calculated cross section [131]. The PYTHIA parameters were subsequently tuned to reproduce these next-to-leading order predictions [131]. For the hadronization of charm and beauty quarks the Lund fragmentation scheme was used [132].

The correlator for pairs of $D\bar{D}$ mesons (left) and $B\bar{B}$ mesons (right) as shown in Fig. 2.7 has a pronounced forward-backward peaked structure. We observe an enhancement at small azimuth from gluon splitting processes, while flavor creation of $c\bar{c}$ -quark pairs leads to an enhanced correlation at backward angles. We have checked that flavor excitation processes lead to a rather flat distribution. To mimic combinatorial background, which

is always present in the experiment, we applied the correlator to D and \bar{D} mesons from different pp collisions, which are physically uncorrelated. This results in a value consistent with zero (see Fig. 2.7). Therefore the correlator allows for a clear distinction between the case where correlations are present (different from zero) or absent (equal to zero)

However, the full kinematic reconstruction of D mesons from topological decays suffers from small branching ratios and rather small reconstruction efficiencies, resulting in low statistics. This is especially the case when pairs of D mesons are considered, as in this case where these factors enter quadratically. As an alternative, we considered electrons (positrons) from the semi-leptonic decays of charm and beauty hadrons, with an average branching ratio to electrons of 10% and 11%, respectively. This clearly indicates that the initial correlations among a heavy quark and its corresponding anti-quark even survive semi-leptonic decays into electrons (positrons) to a large extent.

Further, a comparison of experimental heavy-quark correlations from Pb–Pb collisions to results from microscopic transport calculations would provide an independent way to extract effective heavy-quark scattering rates in the QCD medium [133, 134]. Thus, it might be possible to extract general transport properties, which in turn provide important insight into the microscopic in-medium properties of partons in the QGP and thus the nature of the plasma itself. However, this information would be lost if heavy quarks fully equilibrate with the light partons in the medium.

On the other hand, open heavy-quark correlations also become important in the study of dilepton invariant-mass spectra in high-energy nuclear collisions since the contribution of correlated open heavy-quark decays competes with dilepton emission rates from the QGP in the intermediate invariant-mass range [135–138]. Thus, solid experimental constraints on the extent of the loss of open heavy-quark correlations are essential for an interpretation of the dilepton invariant-mass spectra, in particular concerning mechanisms of chiral symmetry restoration in the hot partonic medium created in high-energy nuclear collisions at LHC energies.

Recently, the CMS Collaboration has measured angular correlations of $B\bar{B}$ mesons with momenta above 15 GeV/ c in pp collisions at $\sqrt{s} = 7$ TeV and found a dominant contribution from gluon splitting processes which is underestimated by calculations in perturbative QCD [139].

3 Outlook

Heavy flavor hadrons carrying a charm or beauty quark are unique probes in modern nuclear and particle physics. Their large mass allows for a quantitative description of their production within perturbative calculations in QCD. A good agreement is found between experiment and theory, within rather large uncertainties in both. Hadronization of charm allows for a description within the Statistical Model. Present experimental results might hint that the contribution from gluon splitting processes to heavy quark production is too low. This might be cured by using a smaller charm mass than is currently assumed in the calculations.

Lead-lead collisions at the highest energies show that charm quark interactions with the QCD medium are substantial. Precise measurements of the phase space distribution of charmed hadrons will address the open question of whether the predicted mass hierarchy of quark energy loss in the hot and dense QCD medium is realized in nature. This addresses the issue of in-medium parton dynamics, which is not yet understood at the fundamental level. Closely related is the medium response to the energy deposit from a heavy quark. The ultrahigh-resolution vertex detectors at the LHC make identification of heavy-quark jets on an event-by-event basis possible. This gives unique access to quark jets, in contrast to gluon jets, which dominate high-momentum particle production at the LHC. At the low momentum side, precise measurements of heavy-quark flow and correlations will decisively address the question of the extent to which heavy quarks participate in the collective expansion of the bulk or even reach kinetic equilibrium. It will then be possible to extract general transport properties, which give an important insight into the microscopic in-medium properties of partons in the QGP, and thus the nature of the plasma itself. However, this information would be lost in the case of heavy quarks fully equilibrating with the light partons in the medium.

These considerations make detection of heavy-quark hadrons down to zero momentum essential, as the topological selection of heavy-quark decays becomes far more challenging in this region. Improved secondary vertexing, in conjunction with excellent particle identification on a track-by-track basis and sophisticated approaches combining information on particle identification from different detectors, e.g. using a Bayesian approach, will help to reduce the combinatorial background and thus extend the accessible momentum

range to the lowest momenta. This will also help in detecting charmed baryons, e.g. Λ_c^+ , which have much shorter lifetimes than the charmed mesons. Also, the relative abundances of charmed hadrons might significantly differ in lead-lead collisions compared to a charm hadronizing in vacuo. In particular, the lifting of strangeness suppression in central lead-lead collisions might alter the role of the strange charmed meson D_s^+ [107]. Full reconstruction of low-momentum B mesons in central lead-lead collisions is limited by low production yields and per mille branching ratios. This might be overcome by yet-increased luminosities being achieved by the accelerator, in combination with faster readout-rate capabilities in the experiments at the LHC.

These goals are within reach in two steps: After the first long shutdown of the LHC, a ten-fold increase in statistics is expected for the second data-taking period starting in 2015. During the second long shutdown foreseen for the whole year of 2018, all experiments will undergo major detector upgrades, including vastly improved secondary-vertexing and readout-rate capabilities. Another increase in statistics of a factor of ten (100 in total) is expected at the high-luminosity LHC.

Complementary to this, charm production close to the threshold and its implications on superdense baryon-rich QCD matter will be studied in (anti)proton-proton, (anti)proton-nucleus and nucleus-nucleus collisions at the Facility for Antiproton and Ion Research (FAIR) currently under construction at the GSI Helmholtz Centre for Heavy-Ion Research, Darmstadt, Germany [140, 141].

References

- [1] X. Zhu *et al.*, *D anti-D correlations as a sensitive probe for thermalization in high-energy nuclear collisions*, Phys.Lett. **B647**, 366 (2007), [arXiv:hep-ph/0604178](#), [doi:10.1016/j.physletb.2007.01.072](#).
- [2] Particle Data Group, J. Beringer *et al.*, *Review of Particle Physics (RPP)*, Phys.Rev. **D86**, 010001 (2012), [doi:10.1103/PhysRevD.86.010001](#).
- [3] Courtesy of J. Mercado, 2013.
- [4] Courtesy of D. Tlusty, 2011.
- [5] BaBar Collaboration, J. Lees *et al.*, *Measurement of the $D^*(2010)^+$ natural line width and the $D^*(2010)^+ - D0$ mass difference*, Phys. Rev. D **88**, **052003** (2013), [arXiv:1304.5009](#), [doi:10.1103/PhysRevD.88.052003](#).
- [6] S. Batsouli, S. Kelly, M. Gyulassy and J. Nagle, *Does the charm flow at RHIC?*, Phys.Lett. **B557**, 26 (2003), [arXiv:nucl-th/0212068](#), [doi:10.1016/S0370-2693\(03\)00175-8](#).
- [7] ALICE Collaboration, K. Aamodt *et al.*, *The ALICE experiment at the CERN LHC*, JINST **3**, S08002 (2008), [doi:10.1088/1748-0221/3/08/S08002](#).
- [8] J. Alme *et al.*, *The ALICE TPC, a large 3-dimensional tracking device with fast readout for ultra-high multiplicity events*, Nucl.Instrum.Meth. **A622**, 316 (2010), [arXiv:1001.1950](#), [doi:10.1016/j.nima.2010.04.042](#).
- [9] A. Akindinov *et al.*, *The commissioning of the ALICE time-of-flight detector and results from the 2008 cosmic-ray data taking*, Nucl.Instrum.Meth. **A615**, 37 (2010), [doi:10.1016/j.nima.2010.01.004](#).
- [10] ALICE Collaboration, K. Aamodt *et al.*, *Alignment of the ALICE Inner Tracking System with cosmic-ray tracks*, JINST **5**, P03003 (2010), [arXiv:1001.0502](#), [doi:10.1088/1748-0221/5/03/P03003](#).

- [11] ALICE Collaboration, B. Abelev *et al.*, *D meson elliptic flow in non-central Pb-Pb collisions at $\sqrt{s_{NN}} = 2.76$ TeV*, Phys.Rev.Lett. **111**, 102301 (2013), arXiv:1305.2707, doi:10.1103/PhysRevLett.111.102301.
- [12] ALICE Collaboration, B. Abelev *et al.*, *D_s^+ meson production at central rapidity in proton-proton collisions at $\sqrt{s} = 7$ TeV*, Phys.Lett. **B718**, 279 (2012), arXiv:1208.1948, doi:10.1016/j.physletb.2012.10.049.
- [13] R. Averbek, *Heavy-flavor production in heavy-ion collisions and implications for the properties of hot QCD matter*, Prog.Part.Nucl.Phys. **70**, 159 (2013), doi:10.1016/j.ppnp.2013.01.001.
- [14] R. Rapp, D. Blaschke and P. Crochet, *Charmonium and bottomonium production in heavy-ion collisions*, Prog.Part.Nucl.Phys. **65**, 209 (2010), arXiv:0807.2470, doi:10.1016/j.ppnp.2010.07.002.
- [15] CDF Collaboration, D. Acosta *et al.*, *Measurement of the J/ψ meson and b -hadron production cross sections in $p\bar{p}$ collisions at $\sqrt{s} = 1960$ GeV*, Phys.Rev. **D71**, 032001 (2005), arXiv:hep-ex/0412071, doi:10.1103/PhysRevD.71.032001.
- [16] M. Cacciari, S. Frixione, M. Mangano, P. Nason and G. Ridolfi, *QCD analysis of first b cross-section data at 1.96-TeV*, JHEP **0407**, 033 (2004), arXiv:hep-ph/0312132, doi:10.1088/1126-6708/2004/07/033.
- [17] B. A. Kniehl, G. Kramer, I. Schienbein and H. Spiesberger, *Finite-mass effects on inclusive B meson hadroproduction*, Phys.Rev. **D77**, 014011 (2008), arXiv:0705.4392, doi:10.1103/PhysRevD.77.014011.
- [18] LHCb Collaboration, R. Aaij *et al.*, *Measurement of $\sigma(pp \rightarrow b\bar{b}X)$ at $\sqrt{s} = 7$ TeV in the forward region*, Phys.Lett. **B694**, 209 (2010), arXiv:1009.2731, doi:10.1016/j.physletb.2010.10.010.
- [19] CMS Collaboration, V. Khachatryan *et al.*, *Prompt and non-prompt J/ψ production in pp collisions at $\sqrt{s} = 7$ TeV*, Eur.Phys.J. **C71**, 1575 (2011), arXiv:1011.4193, doi:10.1140/epjc/s10052-011-1575-8.

- [20] B. Kniehl, G. Kramer, I. Schienbein and H. Spiesberger, *Hadroproduction of D and B mesons in a massive VFNS*, AIP Conf.Proc. **792**, 867 (2005), arXiv:hep-ph/0507068, doi:10.1063/1.2122174.
- [21] B. Kniehl, G. Kramer, I. Schienbein and H. Spiesberger, *Collinear subtractions in hadroproduction of heavy quarks*, Eur.Phys.J. **C41**, 199 (2005), arXiv:hep-ph/0502194, doi:10.1140/epjc/s2005-02200-7.
- [22] M. Cacciari, M. Greco and P. Nason, *The $P(T)$ spectrum in heavy flavor hadroproduction*, JHEP **9805**, 007 (1998), arXiv:hep-ph/9803400.
- [23] M. Cacciari, S. Frixione and P. Nason, *The $p(T)$ spectrum in heavy flavor photoproduction*, JHEP **0103**, 006 (2001), arXiv:hep-ph/0102134.
- [24] CDF Collaboration, D. Acosta *et al.*, *Measurement of prompt charm meson production cross sections in $p\bar{p}$ collisions at $\sqrt{s} = 1.96$ TeV*, Phys.Rev.Lett. **91**, 241804 (2003), arXiv:hep-ex/0307080, doi:10.1103/PhysRevLett.91.241804.
- [25] M. Cacciari and P. Nason, *Charm cross-sections for the Tevatron Run II*, JHEP **0309**, 006 (2003), arXiv:hep-ph/0306212.
- [26] B. Kniehl, G. Kramer, I. Schienbein and H. Spiesberger, *Reconciling open charm production at the Fermilab Tevatron with QCD*, Phys.Rev.Lett. **96**, 012001 (2006), arXiv:hep-ph/0508129, doi:10.1103/PhysRevLett.96.012001.
- [27] ALICE Collaboration, B. Abelev *et al.*, *Measurement of charm production at central rapidity in proton-proton collisions at $\sqrt{s} = 7$ TeV*, JHEP **1201**, 128 (2012), arXiv:1111.1553, doi:10.1007/JHEP01(2012)128.
- [28] ATLAS Collaboration, *Comparison of $D^{(*)}$ meson production cross sections with FONLL and GM-VFNS predictions*, (2011), ATL-PHYS-PUB-2011-012, ATL-COM-PHYS-2011-912.
- [29] LHCb Collaboration, *Prompt charm production in pp collisions at $\sqrt{s} = 7$ TeV*, (2010), LHCb-CONF-2010-013.
- [30] PHENIX Collaboration, A. Adare *et al.*, *Measurement of high- $p(T)$ single electrons from heavy-flavor decays in $p+p$ collisions at $\sqrt{s} = 200$ -GeV*, Phys.Rev.Lett. **97**, 252002 (2006), arXiv:hep-ex/0609010, doi:10.1103/PhysRevLett.97.252002.

- [31] STAR Collaboration, B. Abelev *et al.*, *Erratum: Transverse momentum and centrality dependence of high- p_T non-photonic electron suppression in Au+Au collisions at $\sqrt{s_{NN}} = 200$ GeV*, Phys.Rev.Lett. **98**, 192301 (2007), arXiv:nucl-ex/0607012, doi:10.1103/PhysRevLett.106.159902, 10.1103/PhysRevLett.98.192301.
- [32] M. Cacciari *et al.*, *Theoretical predictions for charm and bottom production at the LHC*, JHEP **1210**, 137 (2012), arXiv:1205.6344, doi:10.1007/JHEP10(2012)137.
- [33] B. Kniehl, G. Kramer, I. Schienbein and H. Spiesberger, *Inclusive Charmed-Meson Production at the CERN LHC*, Eur.Phys.J. **C72**, 2082 (2012), arXiv:1202.0439, doi:10.1140/epjc/s10052-012-2082-2.
- [34] A. Andronic, F. Beutler, P. Braun-Munzinger, K. Redlich and J. Stachel, *Statistical hadronization of heavy flavor quarks in elementary collisions: Successes and failures*, Phys.Lett. **B678**, 350 (2009), arXiv:0904.1368, doi:10.1016/j.physletb.2009.06.051.
- [35] A. Andronic, P. Braun-Munzinger, K. Redlich and J. Stachel, *Evidence for charmonium generation at the phase boundary in ultra-relativistic nuclear collisions*, Phys.Lett. **B652**, 259 (2007), arXiv:nucl-th/0701079, doi:10.1016/j.physletb.2007.07.036.
- [36] Y. L. Dokshitzer and D. Kharzeev, *Heavy quark colorimetry of QCD matter*, Phys.Lett. **B519**, 199 (2001), arXiv:hep-ph/0106202, doi:10.1016/S0370-2693(01)01130-3.
- [37] P. M. Nadolsky *et al.*, *Implications of CTEQ global analysis for collider observables*, Phys.Rev. **D78**, 013004 (2008), arXiv:0802.0007, doi:10.1103/PhysRevD.78.013004.
- [38] CLEO Collaboration, D. Bortoletto *et al.*, *Charm Production in Nonresonant $e^+ e^-$ Annihilations at $\sqrt{s} = 10.55$ GeV*, Phys.Rev. **D37**, 1719 (1988), doi:10.1103/PhysRevD.37.1719, 10.1103/PhysRevD.39.1471.

- [39] ALEPH Collaboration, R. Barate *et al.*, *Study of charm production in Z decays*, Eur.Phys.J. **C16**, 597 (2000), arXiv:hep-ex/9909032, doi:10.1007/s100520000421.
- [40] CDF Collaboration, note 6623, 2003.
- [41] STAR Collaboration, M. Calderon de la Barca Sanchez *et al.*, *Open charm production from d + Au collisions in STAR*, Eur.Phys.J. **C43**, 187 (2005), doi:10.1140/epjc/s2005-02304-0.
- [42] A. David, *Is the fragmentation of charm quarks into D mesons described by heavy quark effective theory?*, Phys.Lett. **B644**, 224 (2007), doi:10.1016/j.physletb.2006.10.071.
- [43] ALICE Collaboration, B. Abelev *et al.*, *Measurement of charm production at central rapidity in proton-proton collisions at $\sqrt{s} = 2.76$ TeV*, JHEP **1207**, 191 (2012), arXiv:1205.4007, doi:10.1007/JHEP07(2012)191.
- [44] C. Buchanan and S. Chun, *A simple predictive model for flavor production in hadronization*, Phys.Rev.Lett. **59**, 1997 (1987), doi:10.1103/PhysRevLett.59.1997.
- [45] F. Becattini, *A Thermodynamical approach to hadron production in e+ e- collisions*, Z.Phys. **C69**, 485 (1996), doi:10.1007/s002880050051.
- [46] R. Rapp and E. Shuryak, *D meson production from recombination in hadronic collisions*, Phys.Rev. **D67**, 074036 (2003), arXiv:hep-ph/0301245, doi:10.1103/PhysRevD.67.074036.
- [47] C. Lourenco and H. Wohri, *Heavy flavour hadro-production from fixed-target to collider energies*, Phys.Rept. **433**, 127 (2006), arXiv:hep-ph/0609101, doi:10.1016/j.physrep.2006.05.005.
- [48] STAR Collaboration, L. Adamczyk *et al.*, *Measurements of D^0 and D^* Production in p + p Collisions at $\sqrt{s} = 200$ GeV*, Phys.Rev. **D86**, 072013 (2012), arXiv:1204.4244, doi:10.1103/PhysRevD.86.072013.

- [49] PHENIX Collaboration, A. Adare *et al.*, *Heavy Quark Production in $p + p$ and Energy Loss and Flow of Heavy Quarks in Au+Au Collisions at $\sqrt{s_{NN}} = 200$ GeV*, Phys.Rev. **C84**, 044905 (2011), [arXiv:1005.1627](#), [doi:10.1103/PhysRevC.84.044905](#).
- [50] M. L. Mangano, P. Nason and G. Ridolfi, *Heavy quark correlations in hadron collisions at next-to-leading order*, Nucl.Phys. **B373**, 295 (1992), [doi:10.1016/0550-3213\(92\)90435-E](#).
- [51] STAR Collaboration, J. Adams *et al.*, *Multiplicity dependence of inclusive p_T spectra from p - p collisions at $\sqrt{s} = 200$ GeV*, Phys. Rev. **D 74**, 17 (2006).
- [52] H1 Collaboration, ZEUS Collaboration, H. Abramowicz *et al.*, *Combination and QCD Analysis of Charm Production Cross Section Measurements in Deep-Inelastic ep Scattering at HERA*, Eur.Phys.J. **C73**, 2311 (2013), [arXiv:1211.1182](#), [doi:10.1140/epjc/s10052-013-2311-3](#).
- [53] D0 Collaboration, V. M. Abazov *et al.*, *Measurement of associated production of Z bosons with charm quark jets in $p\bar{p}$ collisions at $\sqrt{s} = 1.96$ TeV*, 1308.4384, [arXiv:1308.4384](#).
- [54] D0 Collaboration, V. M. Abazov *et al.*, *Measurement of the differential photon + c -jet cross section and the ratio of differential photon+ c and photon+ b cross sections in proton-antiproton collisions at $\sqrt{s} = 1.96$ TeV*, Phys.Lett. **B719**, 354 (2013), [arXiv:1210.5033](#), [doi:10.1016/j.physletb.2013.01.033](#).
- [55] CDF Collaboration, T. Aaltonen *et al.*, *Measurement of the cross section for direct-photon production in association with a heavy quark in $p\bar{p}$ collisions at $\sqrt{s} = 1.96$ TeV*, Phys.Rev.Lett. **111**, 042003 (2013), [arXiv:1303.6136](#), [doi:10.1103/PhysRevLett.111.042003](#).
- [56] CMS Collaboration, *Measurement of associated charm production in W final states at $\sqrt{s} = 7$ TeV*, CMS-PAS-SMP-12-002.
- [57] P. Braun-Munzinger, *Quarkonium production in ultra-relativistic nuclear collisions: Suppression versus enhancement*, J.Phys. **G34**, S471 (2007), [arXiv:nucl-th/0701093](#), [doi:10.1088/0954-3899/34/8/S36](#).

- [58] M. Gyulassy and M. Plümer, *Jet quenching in dense matter*, Phys.Lett. **B243**, 432 (1990), doi:10.1016/0370-2693(90)91409-5.
- [59] R. Baier, Y. L. Dokshitzer, A. H. Mueller, S. Peigne and D. Schiff, *Radiative energy loss and $p(T)$ broadening of high-energy partons in nuclei*, Nucl.Phys. **B484**, 265 (1997), arXiv:hep-ph/9608322, doi:10.1016/S0550-3213(96)00581-0.
- [60] E. Braaten and M. H. Thoma, *Energy loss of a heavy quark in the quark - gluon plasma*, Phys.Rev. **D44**, 2625 (1991), doi:10.1103/PhysRevD.44.2625.
- [61] R. K. Ellis, W. J. Stirling and B. Webber, *QCD and collider physics*, Camb.Monogr.Part.Phys.Nucl.Phys.Cosmol. **8**, 79 (1996).
- [62] N. Armesto, C. A. Salgado and U. A. Wiedemann, *Medium induced gluon radiation off massive quarks fills the dead cone*, Phys.Rev. **D69**, 114003 (2004), arXiv:hep-ph/0312106, doi:10.1103/PhysRevD.69.114003.
- [63] M. Djordjevic and M. Gyulassy, *Heavy quark radiative energy loss in QCD matter*, Nucl.Phys. **A733**, 265 (2004), arXiv:nucl-th/0310076, doi:10.1016/j.nuclphysa.2003.12.020.
- [64] B.-W. Zhang, E. Wang and X.-N. Wang, *Heavy quark energy loss in nuclear medium*, Phys.Rev.Lett. **93**, 072301 (2004), arXiv:nucl-th/0309040, doi:10.1103/PhysRevLett.93.072301.
- [65] S. Wicks, W. Horowitz, M. Djordjevic and M. Gyulassy, *Heavy quark jet quenching with collisional plus radiative energy loss and path length fluctuations*, Nucl.Phys. **A783**, 493 (2007), arXiv:nucl-th/0701063, doi:10.1016/j.nuclphysa.2006.11.102.
- [66] A. Adil and I. Vitev, *Collisional dissociation of heavy mesons in dense QCD matter*, Phys.Lett. **B649**, 139 (2007), arXiv:hep-ph/0611109, doi:10.1016/j.physletb.2007.03.050.
- [67] R. Sharma, I. Vitev and B.-W. Zhang, *Light-cone wave function approach to open heavy flavor dynamics in QCD matter*, Phys.Rev. **C80**, 054902 (2009), arXiv:0904.0032, doi:10.1103/PhysRevC.80.054902.

- [68] H. van Hees, V. Greco and R. Rapp, *Heavy-quark probes of the quark-gluon plasma at RHIC*, Phys.Rev. **C73**, 034913 (2006), arXiv:nucl-th/0508055, doi:10.1103/PhysRevC.73.034913.
- [69] ALICE Collaboration, B. Abelev *et al.*, *Suppression of high transverse momentum D mesons in central Pb-Pb collisions at $\sqrt{s_{NN}} = 2.76$ TeV*, JHEP **1209**, 112 (2012), arXiv:1203.2160, doi:10.1007/JHEP09(2012)112.
- [70] N. Armesto, A. Dainese, C. A. Salgado and U. A. Wiedemann, *Testing the color charge and mass dependence of parton energy loss with heavy-to-light ratios at RHIC and CERN LHC*, Phys.Rev. **D71**, 054027 (2005), arXiv:hep-ph/0501225, doi:10.1103/PhysRevD.71.054027.
- [71] J. Pumplin *et al.*, *New generation of parton distributions with uncertainties from global QCD analysis*, JHEP **0207**, 012 (2002), arXiv:hep-ph/0201195.
- [72] K. Eskola, H. Paukkunen and C. Salgado, *EPS09: A New Generation of NLO and LO Nuclear Parton Distribution Functions*, JHEP **0904**, 065 (2009), arXiv:0902.4154, doi:10.1088/1126-6708/2009/04/065.
- [73] ALICE Collaboration, B. Abelev *et al.*, *Centrality Dependence of Charged Particle Production at Large Transverse Momentum in Pb-Pb Collisions at $\sqrt{s_{NN}} = 2.76$ TeV*, Phys.Lett. **B720**, 52 (2013), arXiv:1208.2711, doi:10.1016/j.physletb.2013.01.051.
- [74] CMS Collaboration, S. Chatrchyan *et al.*, *Suppression of non-prompt J/ψ , prompt J/ψ , and $Y(1S)$ in PbPb collisions at $\sqrt{s_{NN}} = 2.76$ TeV*, JHEP **1205**, 063 (2012), arXiv:1201.5069, doi:10.1007/JHEP05(2012)063.
- [75] Y. He, I. Vitev and B.-W. Zhang, *$\mathcal{O}(\alpha_s^3)$ Analysis of Inclusive Jet and di-Jet Production in Heavy Ion Reactions at the Large Hadron Collider*, Phys.Lett. **B713**, 224 (2012), arXiv:1105.2566, doi:10.1016/j.physletb.2012.05.054.
- [76] W. Horowitz and M. Gyulassy, *Quenching and Tomography from RHIC to LHC*, J.Phys. **G38**, 124114 (2011), arXiv:1107.2136, doi:10.1088/0954-3899/38/12/124114.

- [77] W. Horowitz, *Testing pQCD and AdS/CFT Energy Loss at RHIC and LHC*, AIP Conf.Proc. **1441**, 889 (2012), arXiv:1108.5876, doi:10.1063/1.3700710.
- [78] W. Alberico *et al.*, *Heavy-flavour spectra in high energy nucleus-nucleus collisions*, Eur.Phys.J. **C71**, 1666 (2011), arXiv:1101.6008, doi:10.1140/epjc/s10052-011-1666-6.
- [79] P. Gossiaux, J. Aichelin, T. Gousset and V. Guiho, *Competition of Heavy Quark Radiative and Collisional Energy Loss in Deconfined Matter*, J.Phys. **G37**, 094019 (2010), arXiv:1001.4166, doi:10.1088/0954-3899/37/9/094019.
- [80] O. Fochler, J. Uphoff, Z. Xu and C. Greiner, *Jet quenching and elliptic flow at RHIC and LHC within a pQCD-based partonic transport model*, J.Phys. **G38**, 124152 (2011), arXiv:1107.0130, doi:10.1088/0954-3899/38/12/124152.
- [81] A. Buzzatti and M. Gyulassy, *Jet Flavor Tomography of Quark Gluon Plasmas at RHIC and LHC*, Phys.Rev.Lett. **108**, 022301 (2012), arXiv:1106.3061, doi:10.1103/PhysRevLett.108.022301.
- [82] K. C. Zapp, F. Krauss and U. A. Wiedemann, *A perturbative framework for jet quenching*, JHEP **1303**, 080 (2013), arXiv:1212.1599, doi:10.1007/JHEP03(2013)080.
- [83] J. M. Maldacena, *The Large N limit of superconformal field theories and supergravity*, Adv.Theor.Math.Phys. **2**, 231 (1998), arXiv:hep-th/9711200.
- [84] J. J. Friess, S. S. Gubser, G. Michalogiorgakis and S. S. Pufu, *The Stress tensor of a quark moving through N=4 thermal plasma*, Phys.Rev. **D75**, 106003 (2007), arXiv:hep-th/0607022, doi:10.1103/PhysRevD.75.106003.
- [85] ALICE Collaboration, K. Aamodt *et al.*, *Elliptic flow of charged particles in Pb-Pb collisions at 2.76 TeV*, Phys.Rev.Lett. **105**, 252302 (2010), arXiv:1011.3914, doi:10.1103/PhysRevLett.105.252302.
- [86] ALICE Collaboration, K. Aamodt *et al.*, *Higher harmonic anisotropic flow measurements of charged particles in Pb-Pb collisions at $\sqrt{s_{NN}}=2.76$ TeV*, Phys.Rev.Lett. **107**, 032301 (2011), arXiv:1105.3865, doi:10.1103/PhysRevLett.107.032301.

- [87] J.-Y. Ollitrault, *Anisotropy as a signature of transverse collective flow*, Phys.Rev. **D46**, 229 (1992), doi:10.1103/PhysRevD.46.229.
- [88] P. F. Kolb and U. W. Heinz, *Hydrodynamic description of ultrarelativistic heavy ion collisions*, in *Quark gluon plasma*, edited by R. C. Hwa, pp. 634–714, 2003, arXiv:nucl-th/0305084.
- [89] U. W. Heinz, *Early collective expansion: Relativistic hydrodynamics and the transport properties of QCD matter*, in *Relativistic Heavy Ion Physics*, edited by R. Stock, Landolt-Boernstein New Series, I/23, Springer Verlag, 2010, arXiv:0901.4355.
- [90] M. Gyulassy, I. Vitev and X. Wang, *High $p(T)$ azimuthal asymmetry in noncentral $A+A$ at RHIC*, Phys.Rev.Lett. **86**, 2537 (2001), arXiv:nucl-th/0012092, doi:10.1103/PhysRevLett.86.2537.
- [91] E. Shuryak, *The Azimuthal asymmetry at large $p(t)$ seem to be too large for a ‘jet quenching’*, Phys.Rev. **C66**, 027902 (2002), arXiv:nucl-th/0112042, doi:10.1103/PhysRevC.66.027902.
- [92] STAR Collaboration, K. Ackermann *et al.*, *Elliptic flow in Au + Au collisions at $(S(NN))^{1/2} = 130$ GeV*, Phys.Rev.Lett. **86**, 402 (2001), arXiv:nucl-ex/0009011, doi:10.1103/PhysRevLett.86.402.
- [93] M. Luzum and P. Romatschke, *Viscous Hydrodynamic Predictions for Nuclear Collisions at the LHC*, Phys.Rev.Lett. **103**, 262302 (2009), arXiv:0901.4588, doi:10.1103/PhysRevLett.103.262302.
- [94] CMS Collaboration, S. Chatrchyan *et al.*, *Measurement of the elliptic anisotropy of charged particles produced in PbPb collisions at nucleon-nucleon center-of-mass energy = 2.76 TeV*, Phys.Rev. **C87**, 014902 (2013), arXiv:1204.1409, doi:10.1103/PhysRevC.87.014902.
- [95] ATLAS Collaboration, G. Aad *et al.*, *Measurement of the pseudorapidity and transverse momentum dependence of the elliptic flow of charged particles in lead-lead collisions at $\sqrt{s_{NN}} = 2.76$ TeV with the ATLAS detector*, Phys.Lett. **B707**, 330 (2012), arXiv:1108.6018, doi:10.1016/j.physletb.2011.12.056.

- [96] CMS Collaboration, S. Chatrchyan *et al.*, *Azimuthal anisotropy of charged particles at high transverse momenta in PbPb collisions at $\sqrt{s_{NN}} = 2.76$ TeV*, Phys.Rev.Lett. **109**, 022301 (2012), arXiv:1204.1850, doi:10.1103/PhysRevLett.109.022301.
- [97] ALICE Collaboration, B. Abelev *et al.*, *Anisotropic flow of charged hadrons, pions and (anti-)protons measured at high transverse momentum in Pb-Pb collisions at $\sqrt{s_{NN}}=2.76$ TeV*, Phys.Lett.B **719**, 18 (2013), arXiv:1205.5761, doi:10.1016/j.physletb.2012.12.066.
- [98] V. Greco, C. Ko and R. Rapp, *Quark coalescence for charmed mesons in ultra-relativistic heavy ion collisions*, Phys.Lett. **B595**, 202 (2004), arXiv:nucl-th/0312100, doi:10.1016/j.physletb.2004.06.064.
- [99] G. D. Moore and D. Teaney, *How much do heavy quarks thermalize in a heavy ion collision?*, Phys.Rev. **C71**, 064904 (2005), arXiv:hep-ph/0412346, doi:10.1103/PhysRevC.71.064904.
- [100] D. Molnar and S. A. Voloshin, *Elliptic flow at large transverse momenta from quark coalescence*, Phys.Rev.Lett. **91**, 092301 (2003), arXiv:nucl-th/0302014, doi:10.1103/PhysRevLett.91.092301.
- [101] V. Greco, C. Ko and P. Levai, *Parton coalescence at RHIC*, Phys.Rev. **C68**, 034904 (2003), arXiv:nucl-th/0305024, doi:10.1103/PhysRevC.68.034904.
- [102] ALICE Collaboration, E. Abbas *et al.*, *J/ψ Elliptic Flow in Pb-Pb Collisions at $\sqrt{s_{NN}}=2.76$ TeV*, 1303.5880, arXiv:1303.5880.
- [103] Y. Liu, N. Xu and P. Zhuang, *J/ψ elliptic flow in relativistic heavy ion collisions*, Nucl.Phys. **A834**, 317C (2010), arXiv:0910.0959, doi:10.1016/j.nuclphysa.2010.01.008.
- [104] X. Zhao, A. Emerick and R. Rapp, *In-Medium Quarkonia at SPS, RHIC and LHC*, Nucl.Phys.A904-905 **2013**, 611c (2013), arXiv:1210.6583, doi:10.1016/j.nuclphysa.2013.02.088.

- [105] J. Aichelin, P. Gossiaux and T. Gousset, *Radiative and Collisional Energy Loss of Heavy Quarks in Deconfined Matter*, Acta Phys.Polon. **B43**, 655 (2012), arXiv:1201.4192, doi:10.5506/APhysPolB.43.655.
- [106] J. Uphoff, O. Fochler, Z. Xu and C. Greiner, *Elliptic Flow and Energy Loss of Heavy Quarks in Ultra-Relativistic heavy Ion Collisions*, Phys.Rev. **C84**, 024908 (2011), arXiv:1104.2295, doi:10.1103/PhysRevC.84.024908.
- [107] M. He, R. J. Fries and R. Rapp, *D_s -Meson as Quantitative Probe of Diffusion and Hadronization in Nuclear Collisions*, Phys.Rev.Lett. **110**, 112301 (2013), arXiv:1204.4442, doi:10.1103/PhysRevLett.110.112301.
- [108] T. Lang, H. van Hees, J. Steinheimer, Y.-P. Yan and M. Bleicher, *Heavy quark transport at RHIC and LHC*, J.Phys.Conf.Ser. **426**, 012032 (2013), arXiv:1212.0696, doi:10.1088/1742-6596/426/1/012032.
- [109] PHENIX Collaboration, S. Adler *et al.*, *Measurement of single electron event anisotropy in Au+Au collisions at $\sqrt{s_{NN}} = 200$ GeV*, Phys.Rev. **C72**, 024901 (2005), arXiv:nucl-ex/0502009, doi:10.1103/PhysRevC.72.024901.
- [110] PHENIX Collaboration, A. Adare *et al.*, *Energy Loss and Flow of Heavy Quarks in Au+Au Collisions at $\sqrt{s_{NN}} = 200$ GeV*, Phys.Rev.Lett. **98**, 172301 (2007), arXiv:nucl-ex/0611018, doi:10.1103/PhysRevLett.98.172301.
- [111] A. M. Poskanzer and S. Voloshin, *Methods for analyzing anisotropic flow in relativistic nuclear collisions*, Phys.Rev. **C58**, 1671 (1998), arXiv:nucl-ex/9805001, doi:10.1103/PhysRevC.58.1671.
- [112] ALEPH Collaboration, D. Buskulic *et al.*, *Measurement of the effective b quark fragmentation function at the Z resonance*, Phys.Lett. **B357**, 699 (1995), doi:10.1016/0370-2693(95)00988-W.
- [113] DELPHI Collaboration, P. Abreu *et al.*, *Measurement of Gamma ($b\bar{b}$) / Gamma (hadrons) using impact parameter measurements and lepton identification*, Z.Phys. **C66**, 323 (1995), doi:10.1007/BF01556358.

- [114] OPAL Collaboration, G. Alexander *et al.*, *A Study of b quark fragmentation into B^0 and B^+ mesons at LEP*, Phys.Lett. **B364**, 93 (1995), doi:10.1016/0370-2693(95)01293-7.
- [115] E791 Collaboration, E. Aitala *et al.*, *Correlations between D and anti- D mesons produced in 500-GeV/c π - nucleon interactions*, Eur.Phys.J.direct **C1**, 4 (1999), arXiv:hep-ex/9809029.
- [116] T. Sjostrand *et al.*, *High-energy physics event generation with PYTHIA 6.1*, Comput.Phys.Commun. **135**, 238 (2001), arXiv:hep-ph/0010017, doi:10.1016/S0010-4655(00)00236-8.
- [117] G. D. Moore and D. Teaney, *How much do heavy quarks thermalize in a heavy ion collision?*, Phys.Rev. **C71**, 064904 (2005), arXiv:hep-ph/0412346, doi:10.1103/PhysRevC.71.064904.
- [118] S. Cao and S. A. Bass, *Thermalization of charm quarks in infinite and finite QGP matter*, Phys.Rev. **C84**, 064902 (2011), arXiv:1108.5101, doi:10.1103/PhysRevC.84.064902.
- [119] M. He, R. J. Fries and R. Rapp, *Thermal Relaxation of Charm in Hadronic Matter*, Phys.Lett. **B701**, 445 (2011), arXiv:1103.6279, doi:10.1016/j.physletb.2011.06.019.
- [120] L. Yan, P. Zhuang and N. Xu, *Charm quark thermalization in quark-gluon plasma*, Int.J.Mod.Phys. **E16**, 2048 (2007), doi:10.1142/S0218301307007441.
- [121] B. Svetitsky and A. Uziel, *Passage of charmed particles through the mixed phase in high-energy heavy ion collisions*, Phys.Rev. **D55**, 2616 (1997), arXiv:hep-ph/9606284, doi:10.1103/PhysRevD.55.2616.
- [122] B. Svetitsky and A. Uziel, *Charm: A Thermometer of the mixed phase*, hep-ph/9709228, arXiv:hep-ph/9709228.
- [123] B. Svetitsky and A. Uziel, *Charm transverse momentum as a thermometer of the quark gluon plasma*, (1997).

- [124] S. A. Voloshin, *Transverse radial expansion in nuclear collisions and two particle correlations*, Phys.Lett. **B632**, 490 (2006), arXiv:nucl-th/0312065, doi:10.1016/j.physletb.2005.11.024.
- [125] M. Nahrgang, J. Aichelin, P. B. Gossiaux and K. Werner, *Azimuthal correlations of heavy quarks in Pb+Pb collisions at LHC ($\sqrt{s} = 2.76$ TeV)*, 1305.3823, arXiv:1305.3823.
- [126] A. M. Adare, M. P. McCumber, J. L. Nagle and P. Romatschke, *Tests of the Quark-Gluon Plasma Coupling Strength at Early Times with Heavy Quarks*, 1307.2188, arXiv:1307.2188.
- [127] B. Svetitsky, *Diffusion of charmed quarks in the quark-gluon plasma*, Phys.Rev. **D37**, 2484 (1988), doi:10.1103/PhysRevD.37.2484.
- [128] M. Golam Mustafa, D. Pal and D. Kumar Srivastava, *Propagation of charm quarks in equilibrating quark - gluon plasma*, Phys.Rev. **C57**, 889 (1998), arXiv:nucl-th/9706001, doi:10.1103/PhysRevC.57.3499, 10.1103/PhysRevC.57.889.
- [129] H. van Hees and R. Rapp, *Thermalization of heavy quarks in the quark-gluon plasma*, Phys.Rev. **C71**, 034907 (2005), arXiv:nucl-th/0412015, doi:10.1103/PhysRevC.71.034907.
- [130] G. Tsileadakis, H. Appelshäuser, K. Schweda and J. Stachel, *Heavy-quark azimuthal momentum correlations as a sensitive probe of thermalization*, Nucl.Phys. **A858**, 86 (2011), arXiv:0908.0427, doi:10.1016/j.nuclphysa.2011.03.013.
- [131] ALICE Collaboration, G. Alessandro *et al.*, *ALICE: Physics performance report, volume II*, J.Phys. **G32**, 1295 (2006), doi:10.1088/0954-3899/32/10/001.
- [132] E. Norrbin and T. Sjostrand, *Production and hadronization of heavy quarks*, Eur.Phys.J. **C17**, 137 (2000), arXiv:hep-ph/0005110, doi:10.1007/s100520000460.
- [133] D. Molnar, *Heavy quarks at RHIC from parton transport theory*, Eur.Phys.J. **C49**, 181 (2007), arXiv:nucl-th/0608069, doi:10.1140/epjc/s10052-006-0127-0.

- [134] M. He, H. van Hees, P. B. Gossiaux, R. J. Fries and R. Rapp, *Relativistic Langevin Dynamics in Expanding Media*, 1305.1425, [arXiv:1305.1425](#).
- [135] CERES/NA45 Collaboration, D. Adamova *et al.*, *Enhanced production of low mass electron pairs in 40-AGeV Pb - Au collisions at the CERN SPS*, *Phys.Rev.Lett.* **91**, 042301 (2003), [arXiv:nucl-ex/0209024](#), [doi:10.1103/PhysRevLett.91.042301](#).
- [136] PHENIX Collaboration, A. Adare *et al.*, *Detailed measurement of the e^+e^- pair continuum in $p + p$ and $Au+Au$ collisions at $\sqrt{s_{NN}} = 200$ GeV and implications for direct photon production*, *Phys.Rev.* **C81**, 034911 (2010), [arXiv:0912.0244](#), [doi:10.1103/PhysRevC.81.034911](#).
- [137] H.-j. Xu *et al.*, *Charm quarks in medium and their contribution to di-electron spectra in relativistic heavy ion collisions*, 1305.7302, [arXiv:1305.7302](#).
- [138] T. Lang, H. van Hees, J. Steinheimer and M. Bleicher, *Dileptons from correlated D - and \bar{D} -meson decays in the invariant mass range of the QGP thermal radiation using the UrQMD hybrid model*, 1305.7377, [arXiv:1305.7377](#).
- [139] CMS Collaboration, C. Grab, *Measurement of B - B bar Angular Correlations at $\sqrt{s} = 7$ TeV with the CMS Experiment*, 1110.4751, CMS-CR-2011-169, [arXiv:1110.4751](#).
- [140] B. Friman *et al.*, editors, *The CBM Physics Book*, Lecture Notes in Physics Vol. 814 (, 2011).
- [141] PANDA Collaboration, M. Lutz *et al.*, *Physics Performance Report for PANDA: Strong Interaction Studies with Antiprotons*, 0903.3905, [arXiv:0903.3905](#).